Transactions of the Korean Nuclear Society Spring Meeting
Jeju, Korea, May 29-30, 2014

A comparative study of MATRA-LMR/FB with CFD on THORS bundle 2B test

Won-Pyo Chang, Jin Yoo, Chi-Woong Choi, Kwi-Suk Ha
Korea Atomic Energy Research Institute
P.O.Box 105, Yuseong, Daejeon, 305-600, Korea
**Corresponding author: wpchang@kaeri.re.kr*

1. Introduction

A serious concern in the SFR design was the potential of an external blockage occurrence, and TIB (Total Instantaneous Blockage) was considered as the most severe of all imaginable blockages. In this respect, the SCARABEE-N in-pile tests [1] were performed between 1983 and 1990 to study the consequences of a hypothetical total instantaneous blockage (TIB) at the entrance of a SFR subassembly at full power as an envelopment blockage case. It was observed in the test that the TIB would rapidly led to sodium boiling and dry-out, steel and fuel melting, and the formation of a local boiling pool of these core materials inside the blocked subassembly. The heat fluxes would grow very rapidly above the threshold for melt-through, which would allow the rapid and complete invasion of the neighboring subassemblies. While unlikely, it is possible. Such accident, however, usually has been dealt with a separate topic and its analysis is out of the MATRA-LMR-FB applicable range. Therefore, it was not an issue of this study.

Another concern regarding to the flow blockage is a partial flow blockage inside a subassembly in the SFR. As high thermal conductivity and boiling temperature of sodium coolant may allow a compact core design with narrow flow channels and high power density in the SFR design, such compactness in the core design could be vulnerable to the partial flow blockage caused by an ingression of damaged fuel debris or foreign obstacles into a subassembly. In the partial flow blockage accident, sodium coolant flow would be disturbed in the vicinity of the blockage, and the affected flow could lead to the degradation of the fuel pin due to local coolant temperature rise. In response to the concern, most of technically leading countries for the SFR design have not only conducted critical experiments [2,3,4,5,6,7], but also developed and used computer codes for the flow blockage analysis [8,9,10].

Although the core coolant may normally flow in the axial direction of the fuel pins in a subassembly, a local strong cross flow is also anticipated at a blockage appearance and recirculation region(s) would emerge in a short downstream distance from the blockage. This is why a sophisticated computer code should be required to analyze such complex thermal-hydraulic phenomena in the pin bundle during the partial flow blockage accident. Recognizing the necessity of a flow blockage analysis code in the SFR design, MATRA-LMR-FB, was developed [11,12]. The MATRA-LMR-FB is a revised version of the MATRA-LMR code, which was developed initially for the application to the core sub-channel analysis of the SFR [13], based on the frame of the COBRA-IV-i code [14]. Some of its models were modified and verified to be eligible for the analysis of the sub-channel blockage in the SFR subassembly with wire-wrapped pins.

Although the MATRA-LMR-FB had been qualified based on available experimental data including a code-to-code comparative analysis [15], it was still hard to say that the level of confidence was enough to apply it to the SFR design with a full satisfaction. Additional studies, therefore, are needed to supplement a qualification of the MATRA-LMR-FB. Previous studies usually have been made on the partial flow blockage which was occurred axially near middle of the bundle. Although such blockage position may be typical, there is still a possibility for the inlet partial blockage like the accident in the Fermi reactor 1966 [16] even with a very low frequency. The qualification effort for such a case should be enlarged. In this respect, the 'THORS bundle 2B' test with 19-rod bundle [2,4] was selected to assess the MATRA-LMR-FB for the inlet blockage case. The test results, however, could not provide detailed information on flow and temperature distributions established over the sub-channels enough to assess the MATRA-LMR-FB prediction capability. For this reason, the CFD (Computational Fluid Dynamics) calculations for a few cases were conducted alternatively to provide supplementary information to the assessment before going into a direct comparison with experimental data, because it could provide more detailed information that could not be obtained from the test results on the flow and temperature profiles in the assembly. A problem of how closely the CFD code simulates the test should remain, but it will be a concern for the next step. The postulation is that as the CFD code describes the field equations mostly using the first principle with less averaging processes and assumptions, it could represent more realistic behavior than the MATRA-LMR-FB. The CFX code was selected as a CFD code.

The objective of the present study is to support the qualification of the MATRA-LMR-FB code for its applicability to the partial flow blockage analysis through a code-to-code comparison analysis with the CFX for the 'THORS bundle 2B' test. Therefore, it must be of interest how closely the MATRA-LMR-FB predicts the anticipating phenomena that simulated with the CFX to the test. The outcome of the present study is sure to provide valuable data to demonstrate the

MATRA-LMR-FB applicability to the partial flow blockage analysis**.** The range of the present study is limited to the test cases of no blockage and a 24 sub-channel blockage with high power and flow.

2. Analysis

2.1 THORS bundle 2B test

2.1.1 Experimental apparatus (Han, 1977)

The THORS bundle 2B test was performed to investigate the thermal-hydraulic effects of subassembly inlet blockages as illustrated in Fig. 1. The electrically

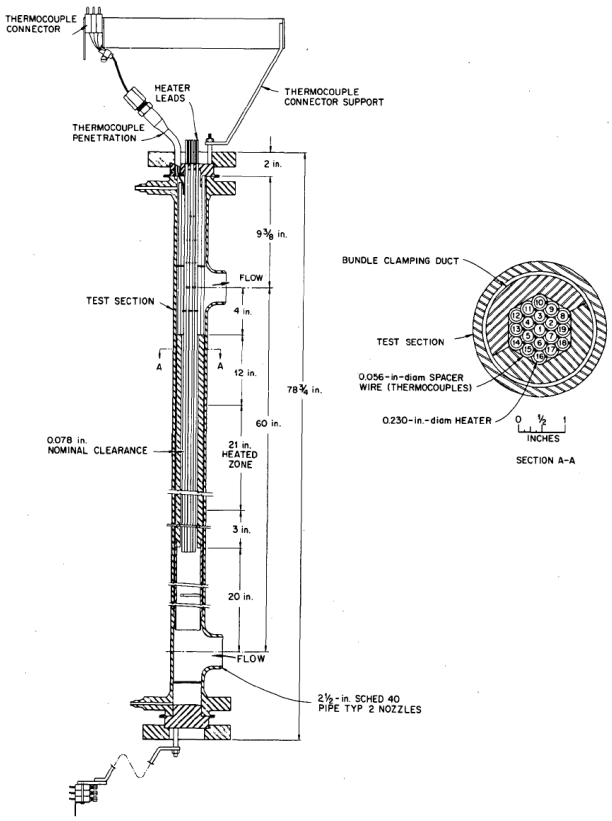

Fig. 1. Test section *for THORS* bundle 2B (Fontana el al., 1977).

heated stainless-steel-clad pins have an outside diameter of 5.84 mm (0.230-in.) and are spaced by 1.42-mm-diameter (0.056-in.) wires, called wire-wraps, which are wound up around the cladding outsides with a 305-mm (12-in.) helical pitch. The distance between the adjacent pin centers (pin pitch) is 7.26 mm (0.286-in.). In the test section (Fig. 3), sodium enters the bundle at the lower end and flows upward. The pins have a heated length of 533 mm (21 in.) preceded by an unheated length of 76.2 mm (3 in.). The stainless steel blockage plate, located at the bottom of the pins, is 1.59 mm (0.0625 in.) thick. Several sub-channels at the same level (i.e. 3-in and 12-in above the heated region) were selected to observe sodium temperature distribution over different sub-channel types (internal, edge, or corner) as well as their radial position. The test was conducted with seven sodium flow-rates with 5 different power levels. The flow rates ranged from 0.69 *l/s* (11 *gpm*) to 3.4 *l/s* (54 *gpm*), while the powers were varied from 16 *kW/m* (5 *kW/ft*) to 6.6 *kW/m* (2 *kW/ft*). The test conditions are summarized in Table 1.

Table 1. Key parameters for the THORS bundle 2B for the input

Parameters	**Unit**	**Inputs**
Number of pins		19
Blockage position		Inlet
Diameter of pin	inch	0.23
Pin pitch	inch	0.286
P/D		1.24
Total length of pin	inch	36
Heated length of pin	inch	21
Wire-wrap pitch	inch	12
Heat flux distribution in the pins		Constant
Diameter of spacer wire	inch	0.056
Flow rates	gpm	11 ~ 54
Power inputs	kW/ft	6.6 ~ 20
Inlet temperature	^{o}F (^{o}C)	600 (316)

2.2 Inputs for the analysis

2.2.1 MATRA-LMR-FB

The cross-section of the bundle arrangement inside the test section is illustrated in Fig. 2. Numberings assigned to the sub-channels as well as rods for the analysis are also indicated. As shown in this figure, the sub-channels can be divided into 3 types depending on their positions inside the hexagonal duct, namely, internal, edge, and corner sub-channels. The internal sub-channel is represented with the sub-channel #1, #2, #3, and so on. An edge sub-channel is surrounded with two rods and the duct, and the sub-channels #25, #26, and so on are examples. A corner sub-channel is the sub-channel located at the corner of the duct e.g. sub-channel #37, #38, and so on. While the bundle inlet was symmetrically blocked covering almost 45% of the total bundle flow area for the 24 sub-channel cases, the blockage was shifted toward a side for the 13 sub-channel blockage occupying about 24 % of the total bundle flow area as seen in Fig. 2. Since the inlet was blocked in the test, the fraction of the total inlet flow which was proportional to the individual sub-channel flow area was allocated at the inlet as a boundary condition, except the blocked sub-channels which have zero flow-rates. The wire-wrap wound up around the rod starting to rotate counterclockwise by 60 degrees azimuthally at the bundle bottom plane. The angle is related with the radial distributions of the flow and temperature in the bundle, because the mixing among the sub-channels largely influenced by the relative angles associated with the appearance of the wire-wrap spacer(s) inside each sub-channel.

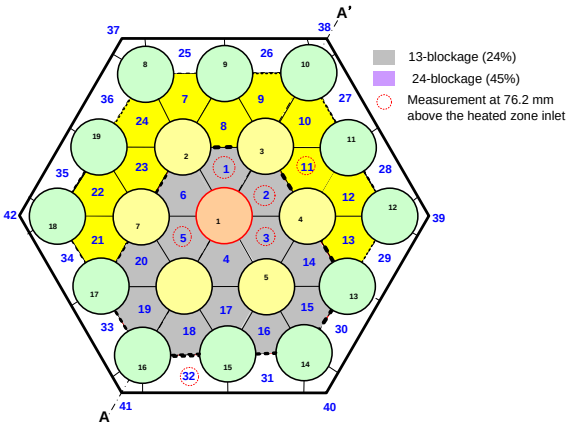

Fig. 2. Cross-sectional configuration of blockages in THORS bundle 2B test.

In the MATRA-LMR-FB input, the sub-channels were divided axially into 36 equally sized nodes (1-inch/node). A preliminary study on node sizes was made to find a suitable size of the node, and a node of 1-inch yielded stable solutions. A constant axial heat flux was given in the heated region with a uniform radial distribution.

2.2.2 CFX

The same boundary conditions as those of the MATRA-LMR-FB with heat flux and inlet flow and outlet pressure of the test were applied to the CFX. The contact between the wire-wrap and the pin rod was modeled with 20 % overlap due to grid generation difficulty but it was not of importance to overall momentum and energy transfer. The k-omega based SST model was selected for turbulent modeling with 5 grid layers for a turbulent sublayer. In addition, the first grid size was defined with y+ of 1. The conjugate heat transfer problem from the cladding to coolant was applied by forcing the heat flux boundary condition at inner surface of the cladding. Table 2 presents the numbers of the optimized nodes and elements over the test assembly in the CFX simulation. The tetrahedral meshes for the free stream region and hexahedral meshes for the boundary layer region were applied to the simulation.

Table 2. Mesh numbers for the CFX calculation

	Node	Element
unblocked	68,314,140	201,714,775
13-inch blocked	61,603,015	190,225,581
24-inch blocked	61,538,050	190,046,504

2.3 Comparison results

The two cases with the high flow (3.4 *l/s*; 54 *gpm*) and the high power (16 *kW/m;*5 *kW/ft*) among the tests were used in the present analyses. They are the cases with no blockage, and a 24 sub-channel blockage which were schematically depicted in Fig. 2. Figure 3 exhibits two colored sub-channel bands (grey and pink colored) lined up in the A-A' direction, and they are subject to representation of the analysis results for the temperature and flow profiles. The dot circled numbers indicate those of experimentally measured sub-channels at 3" above the heating zone entrance.

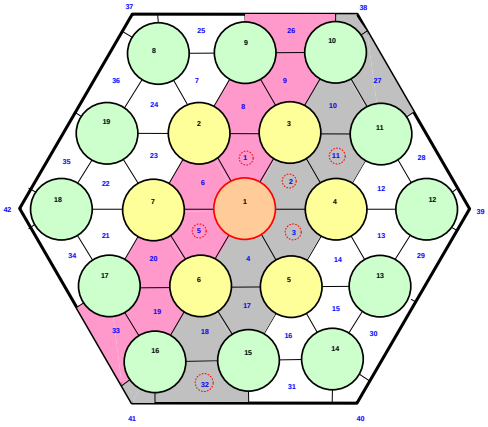

Fig. 3. Sub-channels representing the radial distribution of temperature

2.3.1 No blockage

Figure 4 compares the temperature calculation results at 3" above the heating zone entrance (6" from the bundle bottom) for the case of no blockage. The power input was 5 kW/ft, and the flow was provided with 5 gpm. The temperature predictions by the MATRA-LMR/FB and the CFX codes agreed well with each other. The flows calculated by the two codes were compared in Fig. 5. A small flow discrepancy in the internal sub-channels seemed not to lead to a significant temperature difference, and it conjectured that inter-subassembly coolant mixing would almost uniform in the downstream. Temperatures in the internal sub-channels were calculated much higher than those in the edge and corner sub-channels by both codes. Such a lower temperature in the edge sub-channel mostly attributed to a larger flow area than that of an internal sub-channel.

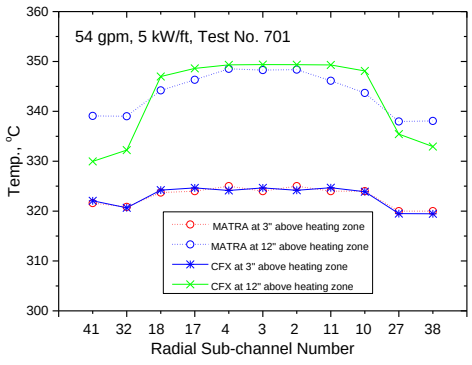

Fig. 4. Comparison of temperature predictions

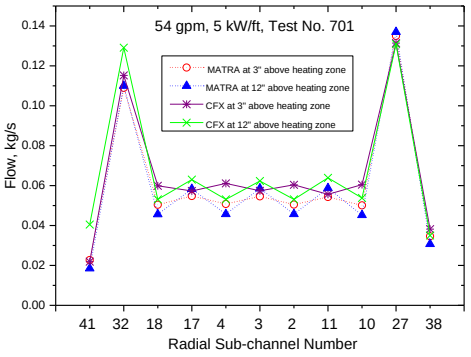

Fig. 5. Comparison of flow predictions

Figure 6 is a visualization of the temperature and the flow distributions along the cross section of A-A' by the MATRA-LMR/FB, and Fig. 7 is a similar exhibition by the CFX. Both results in common showed radially an asymmetric profile in spite of no blockage, primarily due to the asymmetric arrangement of the wire-wrap spacers.

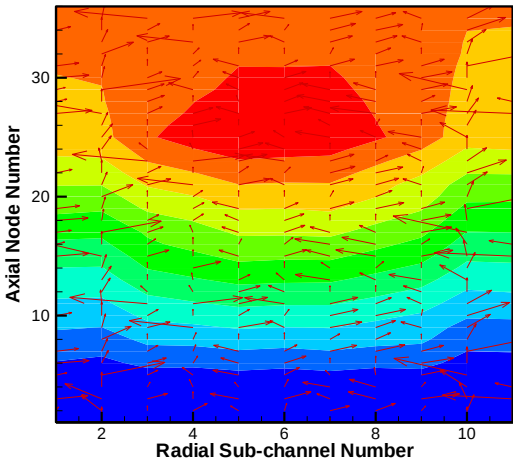

Fig. 6. Temperature and flow distributions along A-A' cross-section (No blockage)

2.3.3 24 sub-channel blockage

The internal sub-channels were blocked evenly in the 24 sub-channel blockage cases as depicted in Fig. 1, and thus the inlet flow passed only through the edge and corner sub-channels at the inlet. The 24-blockage case with 5 gpm and 5 kW/ft (Case No. 740) was analyzed, and the test belongs to a relatively high flow case. Figure 8 compares the temperature predictions by the MATRA-LMR-FB and the CFX in the sub-channels positioned along the cross section of A-A' at 3" above the heated zone entrance along the grey band in Fig. 3. Substantial discrepancies in the temperature predictions were shown even between neighboring sub-channels like #1 and #2. Both predictions were favorably consistent in radial profile as well as in magnitude. However, the prediction of coolant mixing between the neighboring sub-channels by the MATRA-LMR-FB

was conjectured not to be as vigorous as that by the CFX. It was hard to say which prediction would be realistic, because there were no experimental data available for those sub-channels in the grey band at this height.

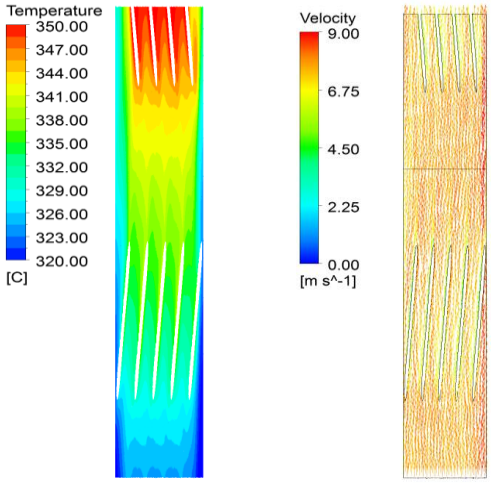

Fig. 7. Temperature and flow distributions along A-A' cross-section from 3" to 12" at the heating zone start (No blockage)

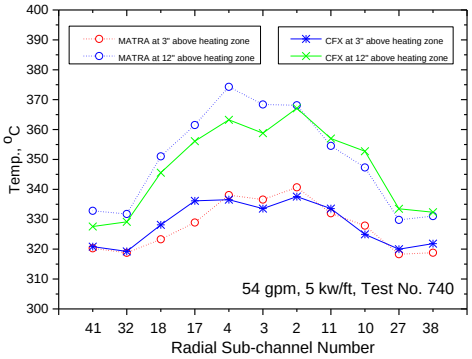

Fig. 8. Temperature comparison for 24-blockge case with 54 gpm (High flow)

The flow distributions predicted by the MATRA-LMR-FB and CFX were represented in Fig. 9. The pattern of the radial distribution was similar to that for no blockage case. Figure 10 illustrates temperature and flow distributions predicted by the MATRA-LMR-FB, and Fig. 11 does those by CFX. A vigorous radial flow movement was revealed near both the edge side sub-channels as expected.

3. Conclusion

The prediction of the MATRA-LMR-FB was compared with that of the CFX with respect to the 'THORS' test. As CFX employs less averaging processes and assumptions, it was believed to represent

the blockage phenomena in more detail. The comparison results generally showed that the two predictions

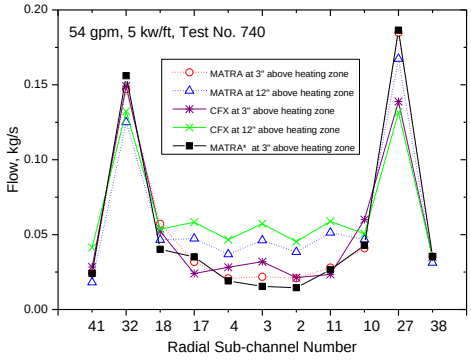

Fig. 9. Comparison of radial flow profiles for 24-blockage case (High flow)

** MATRA*, here, denotes the predictions for the pink colored sub-channel band along the cross-section A-A' in Fig. 3.

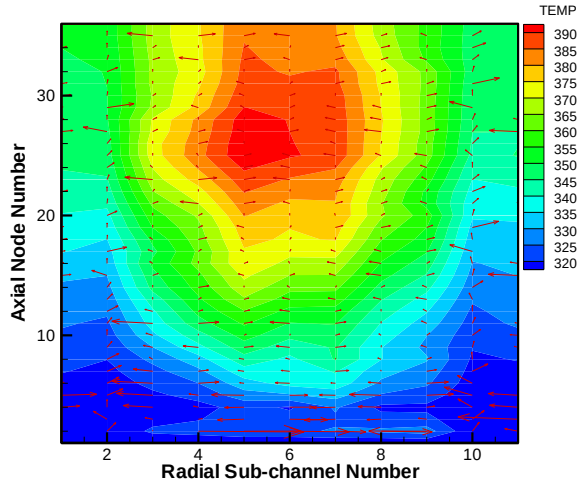

Fig. 10. Temperature and flow distributions along A-A' cross-section

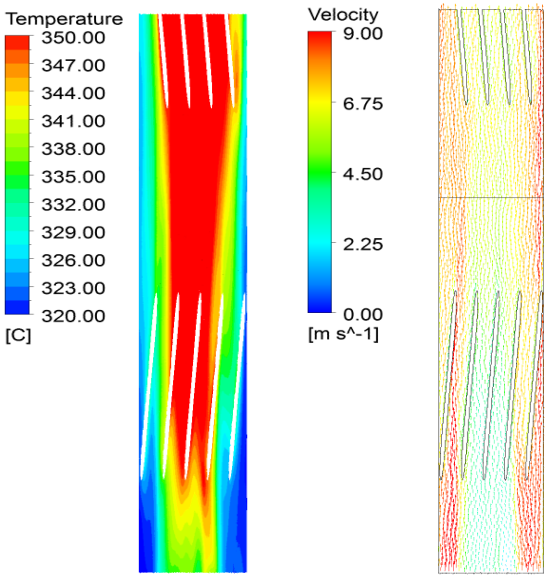

Fig. 11. Temperature and flow distributions from 3" to 12" above the heating entrance for 24 blockage (CFX, High flow)

were consistent both in trend and in magnitude. However, a largest discrepancy of roughly 15 ^{o}C was obtained for the 24 sub-channel blockage case, and it would be elucidated further by comparing with experimental data. The poor coolant mixing between neighboring sub-channels in the radially central region as shown in Fig. 8, was conjectured from the wire-wrap directions in those sub-channels. Therefore, the present results suggest that more investigations on the flow distribution be necessary to evaluate the prediction capability of the MATR-LMR-FB using not only additional cases but also other test results which can provide detailed information on the flow and temperature distributions.

REFERENCES

[1] Kayser, G., Charpenel, J., and Jamond, C., 1998. Summary of the SCARABEE-N subassembly melting and propagation tests with an application to hypothetical total instantaneous blockage in a reactor. Nucl. Sci. Eng. 128, 144–185.

[2] Fontana, M. H. et al., 1973. Effect of partial blockages in simulated LMFBR fuel assemblies, ORNL-TM-4324, Oak Ridge National Laboratory.

[3] Fontana, M. H. et al., 1974. Temperature distribution in the duct wall and at the exit of a 19-rod simulated LMFBR fuel assembly (FFM Bundle 2A)," Nucl. Technol., 24, 176-200.

[4] Han, J. T., 1977. Blockages in LMFBR Fuel Assemblies - A Review of Experimental and Theoretical Studies," ORNL-TM-5839, Oak Ridge National Laboratory.

[5] Haga, K. et al., "Experiments on Local Core Anomaly Detection by Fluctuations of Temperature and Flow Rate at LMFBR Fuel Subassembly Outlets," PNC N 941 81-18, PNC N941 81-74, pp. 5-31 ~ 5-41, PNC, (1981).

[6] Huber, F. and Peppler, W., " Summary and Implications of Out-of-pile Investigations of Local Cooling Distributions in LMFBR Subassembly Geometry under Single-phase and Boiling Conditions," KfK 3927, Kernforschungszentrun Karlsruhe, (1985).

[7] Olive, J. and Jolas, P., "International Blockage in a Fissile Super-Phenix Type Subassembly: The Scarlet Experiments and Their Interpretation by The Cafca-NA3 Code," Nucl. Energy, 4, 287, (1990).

[8] Lin, E. I. H. and Sha, W. T., 1978. Thermal-Hydraulic Analysis of a Wire-Wrapped 19-Rod Bundle with Edge Blockage. Transactions of the ANS 28, 539-540.

[9] Mcdougall, J. D. and Lillington, J. N., 1984. The SABRE Code for Fuel Rod Cluster Thermo Hydraulics. Nucl. Eng. Des. 82, 171.

[10] Ninokata H., et al., 1987. Distributed Resistance Model of Wire-Wrapped Rod Bundles. Nucl. Eng. Des. 104, 93-102.
[11] Ha, K. S., Jeong, H. Y., Chang, W. P., Kwon, Y. M., Cho, C. H., and Lee, Y. B., 2009. Development of the MATRA-LMR-FB for Flow Blockage Analysis in a LMR," Nucl. Eng. Tech. 41, 6, 797-806.
[12] Jeong, H. Y., Ha, K. S., Chang , W. P., Kwon, Y. M., and Lee, Y. B., 2005. Modeling of Flow Blockage in a Liquid Metal–Cooled Reactor Subassembly With a Subchannel Analysis Code. Nuclear Technology 149, 71-87.
[13] Kim, W. S., Kim, Y. K., and Kim, Y. J., 1998. MATRA-LMR Code Development for LMFBR Core Subchannel Analysis. KAERI/TR-1050/98, Korea Atomic Energy Research Institute.
[14] Stewart, C. W., Wheeler, C. L., Cena, R. J., McMonagle, C. Cuta, A. J. M. and Trent, D. S., 1977.
[15] Chang, W.P., Ha, K.S., S.D. Suk, Cheong, H.Y., 2011. A Comparative study of the MATRA-LMR-FB Calculation with the SABRE result for the flow blockage accident in the sodium cooled fast reactor. Nucl. Eng. Des. 241, 5225-5237.
[16] US NRC, 1994. Preapplication Safety Evaluation Report for the Power Reactor Innovative Small Module (PRISM) Liquid-Metal Reactor. NUREG-1368.